JACS
JOURNAL OF THE AMERICAN CHEMICAL SOCIETY

ARTICLE

pubs.acs.org/JACS

Displacement of Hexanol by the Hexanoic Acid Overoxidation Product in Alcohol Oxidation on a Model Supported Palladium Nanoparticle Catalyst

Avram M. Buchbinder,[†,#] Natalie A. Ray,[†] Junling Lu,[‡] Richard P. Van Duyne,[†,#] Peter C. Stair,[†,#,§] Eric Weitz,[†,#] and Franz M. Geiger*[,†,#]

[†]Department of Chemistry, Center for Catalysis and Surface Science and the [#]Institute for Catalysis in Energy Processes, Northwestern University, Evanston, Illinois, 60208

[‡]Energy System Division[§]Chemical Sciences and Engineering Division, Argonne National Laboratory, Argonne, Illinois 60439, United States

Supporting Information

ABSTRACT: This work characterizes the adsorption, structure, and binding mechanism of oxygenated organic species from cyclohexane solution at the liquid/solid interface of optically flat alumina-supported palladium nanoparticle surfaces prepared by atomic layer deposition (ALD). The surface-specific nonlinear optical vibrational spectroscopy, sum-frequency generation (SFG), was used as a probe for adsorption and interfacial molecular structure. 1-Hexanoic acid is an overoxidation product and possible catalyst poison for the aerobic heterogeneous oxidation of 1-hexanol at the liquid/solid interface of Pd/Al_2O_3 catalysts. Single component and competitive adsorption experiments show that 1-hexanoic acid adsorbs to both ALD-prepared alumina surfaces and alumina surfaces with palladium nanoparticles, that were also prepared by ALD, more strongly than does 1-hexanol. Furthermore, 1-hexanoic acid adsorbs with conformational order on ALD-prepared alumina surfaces, but on surfaces with palladium particles the adsorbates exhibit relative disorder at low surface coverage and become more ordered, on average, at higher surface coverage. Although significant differences in binding constant were not observed between surfaces with and without palladium nanoparticles, the palladium particles play an apparent role in controlling adsorbate structures. The disordered adsorption of 1-hexanoic acid most likely occurs on the alumina support, and probably results from modification of binding sites on the alumina, adjacent to the particles. In addition to providing insight on the possibility of catalyst poisoning by the overoxidation product and characterizing changes in its structure that result in only small adsorption energy changes, this work represents a step toward using surface science techniques that bridge the complexity gap between fundamental studies and realistic catalyst models.

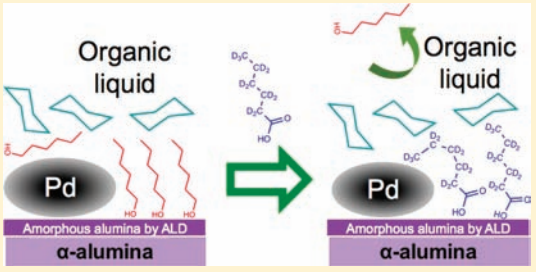

INTRODUCTION

Selective oxidation processes can be heterogeneously catalyzed using oxide-supported metal nanoparticles maintained under an organic solvent.[1−13] In an effort to achieve predictive capabilities for improved catalyst design and performance, a molecular level understanding of the interactions between the adsorbates, the solvent, the catalyst, and its support is needed. While ultrahigh vacuum studies have elucidated molecular adsorption and reaction pathways on pristine single-crystal surfaces with great success,[14−17] few fundamental molecular surface science studies address catalytically relevant surfaces that are in contact with liquids or high-pressure gases.[4,15,18−23] Such studies show that molecular behavior at liquid/solid interfaces differs dramatically from the UHV environment.[18,24−34] These findings are important because even modest changes in the molecular structure can modify reactionz rate and selectivity by modulating activation barriers to reactant adsorption, chemical reaction, and product desorption.[18,35−39]

Here, we demonstrate these concepts for the specific example of poisoning in one of the most extensively studied reactions that takes place at the interface between a nonionic organic liquid and an oxide-supported metal nanoparticle catalyst, namely the heterogeneous selective oxidation of alcohols to aldehydes.[4,5,40] Using vibrational sum frequency generation (SFG),[41−46] we probe the adsorption behavior and molecular level conformational ordering of 1-hexanoic acid, and follow its displacement of 1-hexanol on amorphous alumina surfaces containing Pd nanoparticles prepared by atomic layer deposition (ALD). We elucidate the role of 1-hexanoic acid as a surface poison and show that the presence of palladium particles on an oxide surface results in a molecular-level structural change in 1-hexanoic acid adsorbates.

The heterogeneous selective oxidation of alcohols to aldehydes has been developed as a widely used alternative to homogeneous oxidations requiring environmentally damaging oxidants.[8,47] It possesses additional relevance as a model reaction for other selective oxidations for which improved catalysts are needed.[48−51] The reaction can be carried out at the liquid/solid interface of a supported or grafted palladium or noble metal catalyst with molecular oxygen as the oxidant.[3−6,8,52−55] Extensive research in developing these catalysts has produced exquisite selectivity to aldehydes without overoxidation as measured by the composition of the effluent.[3,5,6,8,47,52−54] However, Baiker

Received: July 28, 2011
Published: September 15, 2011

Scheme 1. Schematic Depicting the Preparation of Surfaces by ALD

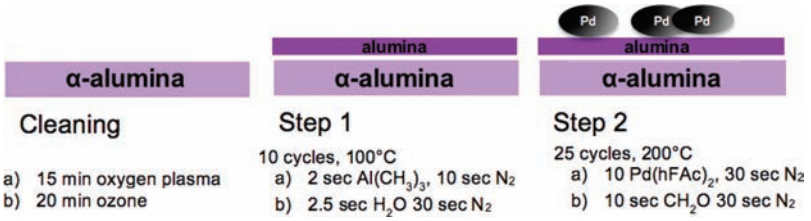

and co-workers have shown that carboxylates or molecularly adsorbed carboxylic acids may be present on the surface and suggest that these species act as catalyst poisons.[4,40,55] The oxide support in these reactions is known to act as a base or oxidant to dehydrogenate the reactant,[4,5] and poisoning it or the metal particles decreases catalyst effectiveness. However, it is not known if a carboxylic acid or carboxylate species hinders the reaction by blocking reactive sites on the metal particles or if it does so on the support. Likewise, it is not known what the concentration threshold is for catalyst poisoning, i.e. what mole fraction of carboxylic acid in the liquid phase shuts down access to adsorption sites for the alcohol reactant.

EXPERIMENTAL APPROACH

In the experiments, we employ ALD (which is a method developed for the preparation of thin, conformal films that has recently been extended to produce operational supported metal nanoparticle catalysts[56−62]) to prepare flat surfaces containing palladium nanoparticles on amorphous alumina (Scheme 1). By characterizing the surfaces with grazing incidence X-ray diffraction (GIXRD) and X-ray photoelectron spectroscopy (XPS), along with previous work using scanning transmission electron microscopy (STEM), scanning electron microscopy (SEM), and quartz crystal microbalance (QCM) measurements,[57,62,63] we determine that the particles have 3 nm diameter with monodisperse size distribution ($\sigma < 1$ nm), supported on 1-nm-thick amorphous alumina at a particle density of $1 - 2 \times 10^{12}$ cm^{-2}. After exposure to the organic liquids used in this work, particles contain some palladium oxide and may increase in average size by a small amount (see Supporting Information). We then use vibrational SFG spectroscopy[26,64−69] to directly probe the alcohol reactant and acid overoxidation product within the anisotropic interfacial region of the ALD substrates in contact with binary and ternary solutions containing cyclohexane solvent.

Materials. α-Al_2O_3 substrates were purchased from MTI crystals (two sides polished, 1 mm thick, 0.5 in. × 0.5 in, C plane), washed and sonicated in methanol, dried under nitrogen, and cleaned in an oxygen plasma cleaner (Herrick) prior to introduction into the ALD chamber, where they were subjected to further ozone treatment before deposition. Trimethylaluminum (97%), palladium hexafluoroacetylacetonate (99%), and formalin (ACS reagent grade), the precursors for ALD, were all obtained from Sigma-Aldrich (Milwaukee, WI). Formalin is composed of 37% formaldehyde and 10−15% methanol in water; methanol acts as a stabilizer to prevent polymerization. Cyclohexane-d_{12} (99.6 atom % D), hexanoic acid (99.5+%), and 1-hexanol were obtained from Aldrich (Milwaukee, WI), while 1-hexanoic-d_{11} acid (98.8 atom % D) was obtained from CDN isotopes (Pointe-Claire, Quebec, Canada).

ALD Reactor. Al_2O_3 and Pd ALD were performed using a viscous flow reactor system similar to one previously described.[70] Ultrahigh-purity nitrogen (99.999%) was used as both the carrier and purge gas with a mass flow rate of 360 sccm. The system pressure was between 1 and 2 Torr. Two precursors, A and B, are alternately dosed and purged through the reactor. The ALD time sequence for one AB cycle can be written as $t_1-t_2-t_3-t_4$ where t_1 is dose time for A, t_2 is purge time for A, t_3 is dose time for B, and t_4 is purge time for B, all in seconds.

Ozone Treatment. After the samples were loaded into the ALD reactor, an *in situ* ozone treatment (Pacific Zone Lab111 ozone generator) was performed at 100 °C for 20 min before beginning ALD to reduce the amount of organic material on the substrate before deposition. Ultrahigh purity oxygen (99.999%), flowing at 200 sccm, was used as the oxygen source. The ozone reactor pressure was maintained at 2 psi, and ozone output was set to 75% at 5.2 V.

ALD Alumina Film Growth. To grow Al_2O_3 using ALD, trimethylaluminum (TMA) and 18.2 MΩ cm^{-1} Millipore water (Marlborough, MA) were alternately dosed and purged at 100 °C. Ten cycles of TMA/H_2O were deposited on the cleaned α-Al_2O_3 substrates using the time sequence 2−10−2.5−30 s resulting in a film 1 nm thick.[58]

ALD Pd Particle Growth. Pd ALD has high nucleation density on amorphous ALD Al_2O_3.[63] Therefore, all α-Al_2O_3 substrates used for Pd ALD were first coated with a layer of ALD Al_2O_3. Pd ALD was grown at 200 °C using palladium hexafluoroacetylacetonate ($Pd(hfac)_2$) and formalin.[57,63] Twenty-five cycles of $Pd(hfac)_2$/HCHO were deposited on the ALD Al_2O_3 surface using the time sequence 10−30−10−30 s. In the early stages of Pd ALD, nanoparticle size is controlled by the number of cycles.[63]

Sum Frequency Generation. Descriptions of SFG[41,42,44,46,71] and the broadband SFG setup used in this work[24,43,72,73] can be found elsewhere. SFG experiments were performed in an internal reflection geometry at room temperature, with the α-Al_2O_3 serving as both a substrate for the ALD surface and an optical window. Directly following sample preparation, the sample was clamped onto a small-volume (0.15 mL) Teflon cell, containing a port for injection and removal of solution.[24,25] The IR and visible laser beams for SFG were focused on the interface between the ALD-modified surface and organic liquid solutions. SFG spectra were collected in the SSP polarization combination, which requires that a component of the IR transition dipole be oriented along the surface normal for signal to be produced.[45,66,74,75] The SFG spectra in this work are the average of seven acquisitions of 90 s each. SFG frequency was calibrated using the IR absorption bands that appear in the SFG spectrum of gold when a polystyrene film was placed in the IR beam path.[76] Following the hybrid scanning−tuning method of Esenturk and Walker,[66] spectra were collected at three different input IR frequencies, and summed together. Where noted, the SFG intensities obtained were then normalized to the nonresonant frequency-dependent intensity of a gold sample (also in internal reflection geometry),[24,43,72,73] and in other cases the spectra shown are not normalized in order to avoid singularities, but the values of intensity obtained from the spectra are appropriately corrected. Spectra were fit with interfering Lorentzian lineshapes plus a small constant nonresonant signal, where each peak was allowed to have a phase of 0° or 180°.[24,43,72,73] Global fitting procedures were employed (using built-in functionality of IGOR-Pro version 4.09A Carbon, WaveMetrics) in which frequency and line width were fit as global variables over all concentrations in order to isolate the amplitudes as the concentration-dependent variables.

RESULTS AND DISCUSSION

Under liquid perdeuterated cyclohexane-d_{12} (cyclohexane-d_{12}), ALD alumina substrates exhibit a small resonant SFG signal due

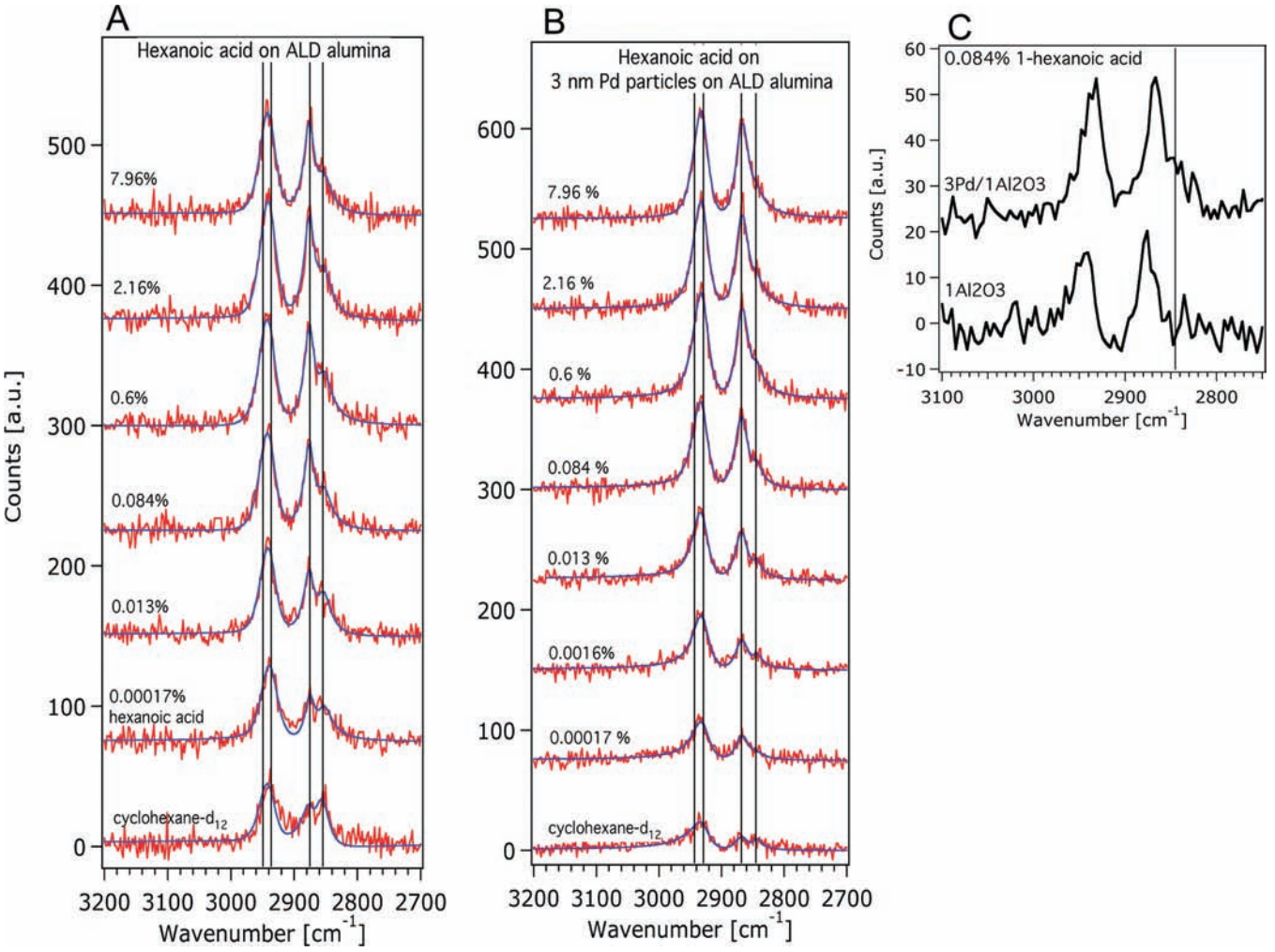

Figure 1. SFG spectra of 1-hexanoic acid adsorbed from liquid cyclohexane-d_{12} solutions onto ALD alumina (A) and ALD alumina with 3 nm palladium particles (B). Fits to the data are shown in blue, and vertical lines mark the frequencies of vibrational bands. The data are not normalized, but the resulting numbers plotted in the figures that follow are normalized to the signal from gold to account for frequency-dependent differences in infrared power. The SFG spectra are shown for 0.084% 1-hexanoic acid on both the ALD alumina surface and ALD alumina with 3 nm palladium particles, normalized to the signal from gold and referenced to the signal without added 1-hexanoic acid (C), with a vertical line marking the contribution from the CH_2 symmetric stretch which is a measure for conformational disorder. This plot shows a direct comparison between the two surfaces.

to a small amount of adventitious organic material acquired in the ALD chamber (see Supporting Information). The invariance of the signal strength with number of ALD cycles indicates that the CH oscillators in the adventitious material are removed by the ALD precursors during each cycle and remain only on the surface upon completion of all deposition cycles, which is in agreement with QCM measurements by Wind and George.[77] Small SFG signal intensities obtained from samples containing palladium particles (see Supporting Information) are attributed to either similar deposition of organic material in the ALD reactor or to formalin, having well-known vibrational bands in the 2800−3000 cm^{-1} region,[60,78] and hexafluoroacetoacetonate (hfac) ligands, as evidenced by F 1s peaks in the XPS spectra, that are used during the ALD process but not quantitatively removed during it. The presence of hfac, formalin, and their derivatives on the surface cause only a very small loss in the number of hydroxyl surface sites, as demonstrated by Goldstein and George using transmission FTIR.[78] These findings point to a means for optimizing ALD procedures using SFG as a sensitive probe for surface species in assessing the quantitative nature of ALD reactions. Despite the SFG signals from adventitious material, its contribution to the SFG signal intensity is much less than that of adsorbed hexanol or 1-hexanoic acid, and 1-hexanoic acid may displace the material upon adsorption (see below). Therefore, we chose not to calcine the materials under investigation here after ALD in order to prevent oxidation, sintering, agglomeration, and changes in morphology of the palladium particles,[14,79] which in turn control adsorption and reactivity on the particles.[80,81]

SFG spectra of binary mixtures of 1-hexanoic acid in cyclohexane-d_{12} on ALD alumina with and without Pd nanoparticles (Figure 1) show vibrational bands that were assigned on the basis of well-established literature data.[38,66−68,71,72,75,82−87] Briefly, the symmetric stretches of the CH_3 and CH_2 groups of the 1-hexanoic acid alkyl tail appear at 2871 cm^{-1} and 2851 cm^{-1}, respectively. The peak at 2933 cm^{-1} is assigned to the CH_3 Fermi resonance, and the peak at 2947 cm^{-1} is assigned to the asymmetric stretch of the CH_3 group. While the CH_2 asymmetric stretch is not well resolved, its amplitude is expected to be low for perpendicularly oriented alkyl chains.

Using the concentration-dependent SFG spectra of hexanoic acid and 1-hexanol,[25] we determined the binding constants for

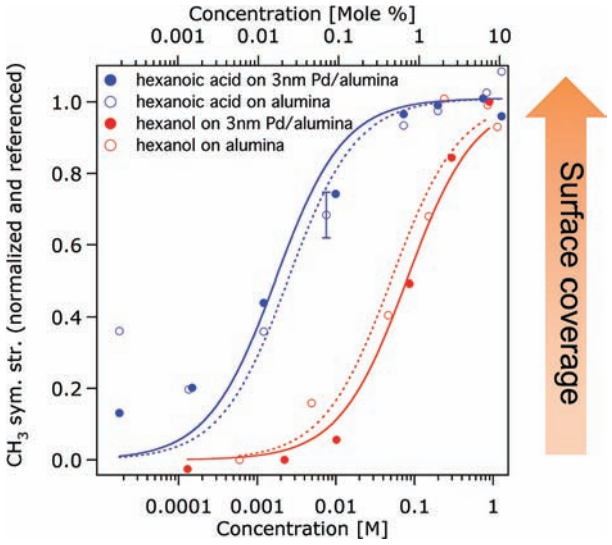

Figure 2. Peak amplitudes of the CH_3 symmetric stretch (markers) and fits of the data to a Langmuir adsorption model (lines) of 1-hexanoic acid on ALD alumina with 3 nm palladium particles (blue filled squares, uneven dashed blue line), 1-hexanoic acid on ALD alumina without palladium particles (blue empty squares, dotted blue line), 1-hexanol on ALD alumina with 3 nm palladium particles (red filled circles, solid red line), and 1-hexanol on ALD alumina without palladium particles (red empty circles, dashed red line), each at the interface of a solution of the analyte in cyclohexane-d_{12}. The peak amplitudes (left axis) are obtained from spectral fitting of SFG spectra as a function of mol % (top axis) and approximate concentration in molar (bottom axis), referenced to signal from the surface under pure cyclohexane-d_{12}, and normalized to saturation coverage. The error bar represents the average reproducibility of SFG peak amplitude.

these two species (Figure 2) from the normalized and properly referenced SFG amplitude of the CH_3 symmetric stretch. The adsorption behavior is certainly more complicated than can be accurately described by the standard Langmuir adsorption model.[88] For instance, a portion of adsorbates may interact with the surface irreversibly,[20,21] the presence of the Pd nanoparticles introduces multiple adsorption sites, and adsorbate−adsorbate interactions are likely present albeit relatively weak when compared to that of longer chain molecules.[20,21,25] Nonetheless, these departures from Langmuirian adsorption are not systematically evident in the data, either because the departures from that model are in opposite directions or simply because SFG is not sensitive enough to detect them. Each SFG measurement was made after the signal reached a constant value, and this work therefore addresses presumed equilibrium behavior rather than the kinetics of adsorption. By fitting each isotherm with the Langmuir adsorption model, we obtain, as a first-order approximation, binding constants K_{ads} for 1-hexanoic acid and 1-hexanol using the fractional coverages in comparison to signal saturation which is normalized to one. We also obtain the associated standard free energies of adsorption, ΔG°_{ads}, referenced to a standard state of 9.28 M, the concentration of pure cyclohexane-d_{12} at 298 K (Table 1). 1-Hexanoic acid adsorbs to both surfaces more strongly than 1-hexanol. Given the error in parameters resulting from fits to the data, this analysis reveals a 8−40-fold difference in K_{ads} between the two adsorbates on ALD alumina, and a 40−60-fold difference in K_{ads} between the two adsorbates on the ALD alumina surface with Pd nanoparticles. This corresponds to a

Table 1. Binding Constants K^*_{ads} and Standard Free Energies of Adsorption ΔG°_{ads} Approximated with a Langmuir Adsorption Model[a]

adsorbate	surface	K^*_{ads} [M^{-1}]	ΔG°_{ads} [kJ mol^{-1}]
1-hexanoic acid	alumina/Pd	6×10^2 (2)	−21.1 (7)
1-hexanoic acid	alumina	4×10^2 (2)	−20. (1)
1-hexanol	alumina/Pd	12 (2)	−11.8 (4)
1-hexanol	alumina	20 (5)	−13.0 (6)

[a] One standard deviation in the last significant figure is listed in parentheses.

5.4−8.6 kJ/mol differece in ΔG°_{ads} between the two adsorbates on ALD alumina and an 8.2−10.4 kJ/mol difference in ΔG°_{ads} between the two adsorbates on ALD alumina with Pd nanoparticles. On the other hand, the comparison of ΔG°_{ads} values between the two surfaces reveals that the presence of Pd nanoparticles does not change ΔG°_{ads} significantly for either adsorbate by more than the uncertainty associated with the experiment, and that the difference between the two surfaces is within the bounds attributable to thermal noise.

In the above result, 1-hexanol and 1-hexanoic were adsorbed separately to the surfaces, and thus adsorption of the two species to entirely separate sites could be ruled out. Thus, to address our central question regarding the molecular origin of catalyst poisoning in selective heterogeneous alcohol oxidation by over-oxidation products, we conducted competitive adsorption experiments in which 1-hexanol was first adsorbed to the surface from a 9% solution in cyclohexane-d_{12}, followed by exposure to solutions with a constant 9% concentration of 1-hexanol, but with increasing amounts of spectrally silent 1-hexanoic acid-d_{11} (Figures 3 and 4). These experiments show that addition of just 0.02 mol % 1-hexanoic acid-d_{11} begins to displace hexanol, half of the hexanol is displaced upon addition of 0.5 mol % 1-hexanoic acid-d_{11}, and all hexanol is removed with addition of 5 mol % 1-hexanoic acid-d_{11}. The competitive adsorption behavior on surfaces both with and without Pd nanoparticles is consistent with a Langmuir competitive adsorption model (shown in Figure 4), which assumes a single type of binding site for 1-hexanoic acid-d_{11} and hexanol. This result emphasizes the significance of catalyst poisoning, since the reactant and overoxidation product compete for the same sites. Note that the process of adding spectrally silent hexnaoic acid-d_{11} results in signal levels that are even lower than the signal produced by adventitious material that was present before adding adsorbates (vide supra). This provides evidence that in addition to displacing hexanol, carboxylic acid species also displace organic material that originated in the ALD chamber or that this material reorients in the presence of hexanoic acid in a fashion that suppresses its SFG response.

The results presented here do not provide evidence pointing to 1-hexanoic acid binding primarily to palladium but rather suggest that hexanol and hexanoic acid adsorb to alumina binding sites, as evidenced by the nearly identical adsorption energies obtained for the organic species on ALD alumina with and without Pd nanoparticles, and the similar displacement of hexanol by hexanoic acid on both surfaces. This result is consistent with studies carried out under aqueous[89] and organic solvent[4,20,21] environments which suggest that 1-hexanoic acid molecules preferentially adsorb to sites on the alumina surface. However, recent results for unsaturated carboxylic acids suggest that palladium plays a role in modulating binding.[90] Experiments

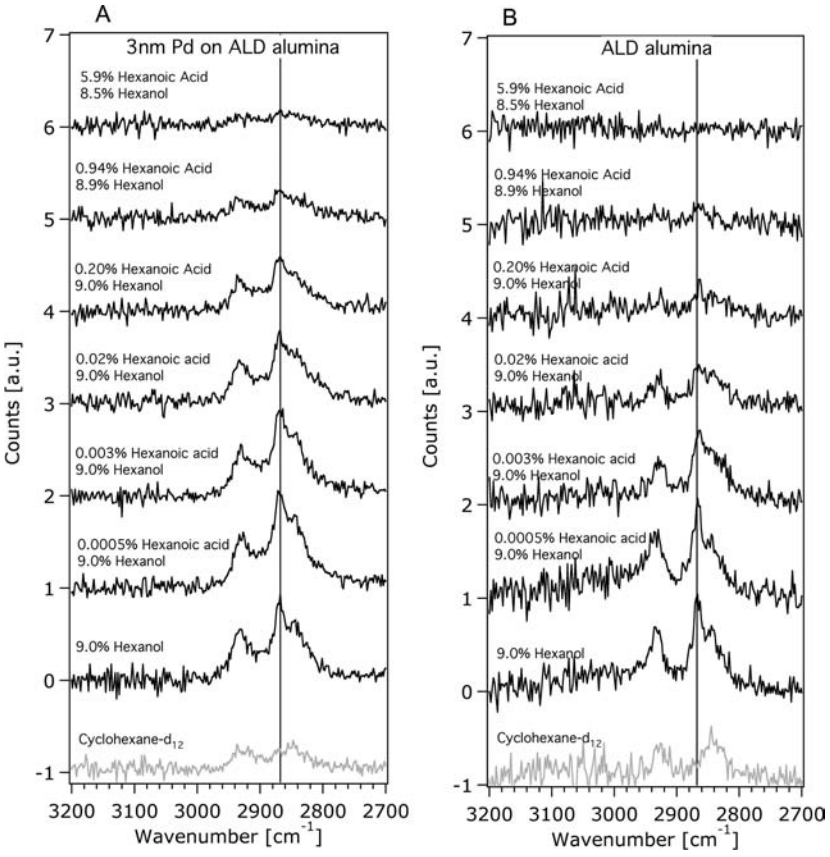

Figure 3. SFG spectra of 9% 1-hexanol in cyclohexane-d_{12} adsorbed on ALD alumina with 3 nm palladium particles (A) and ALD alumina without palladium particles (B), with subsequently added amounts of added 1-hexanoic acid-d_{11}. Spectra are normalized to gold to account for frequency-dependent input power, and to the highest intensity for hexanol signal on that surface to account for differences in laser alignment and power.

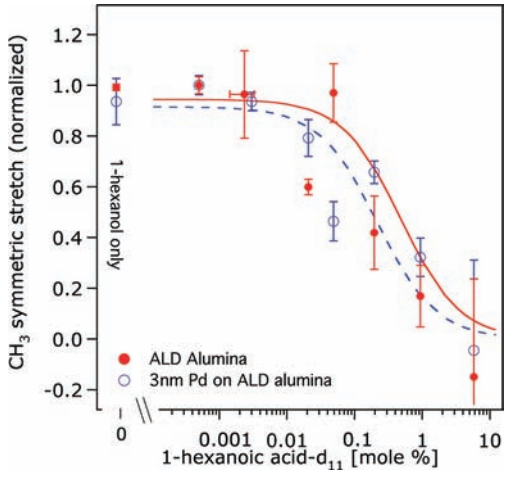

Figure 4. Amplitudes of the CH_3 symmetric stretch peak in the SFG spectra of 1-hexanol in cyclohexane-d_{12} are plotted as a function of added 1-hexanoic acid-d_{11} mol % on the ALD alumina surface (red filled circles) and on ALD alumina with 3 nm palladium particles (blue empty circles). Competitive adsorption models derived from the independently measured K_{ads} values of the two species on the ALD alumina surface (solid red line) and the independently measured K_{ads} values of the two species on ALD alumina with 3 nm palladium particles (dashed blue line) are plotted for comparison.

on a surface fully covered with palladium would be necessary to confirm that binding occurs on alumina rather than palladium sites; however, samples with palladium loading equivalent to full coverage prepared either by ALD or by an electron beam result in SFG spectra dominated by nonresonant response of the metal with no resonant signals from adsorbates upon 1-hexanoic acid addition (see Supporting Information).

Despite the lack of a significant difference in ΔG°_{ads} for 1-hexanoic acid on surfaces with and without palladium particles, the molecular conformation that it adopts in the presence of nanoparticles could nonetheless indicate a measurable interaction with palladium. The ratio of the CH_3 symmetric stretching signal to the CH_2 symmetric stretching signal, which is often used as measure of molecular ordering,[25,26,66−69] shows that the conformational order increases dramatically as a function of 1-hexanoic acid concentration when the Pd nanoparticles are present (except at concentration >10 mol % where there is a decrease, probably due to formation of multilayer structures[25]), while very little change in this ratio is observed when Pd particles are absent (Figure 5). On the surfaces with no palladium particles, on which no change in conformational ordering is observed, 1-hexanoic acid is likely adsorbing in an ordered manner on the large domains of uninterrupted alumina. In contrast, on the surfaces with palladium particles, the low degree of conformational order at low surface coverages implies interaction with the nanoparticles that causes only small changes in adsorption energy and is otherwise undetectable without a surface-specific probe for molecular structure.

Several types of interactions may lead to disordered adsorption of 1-hexanoic acid on surfaces with palladium nanoparticles. Given that the coordination strength of carboxylate to the

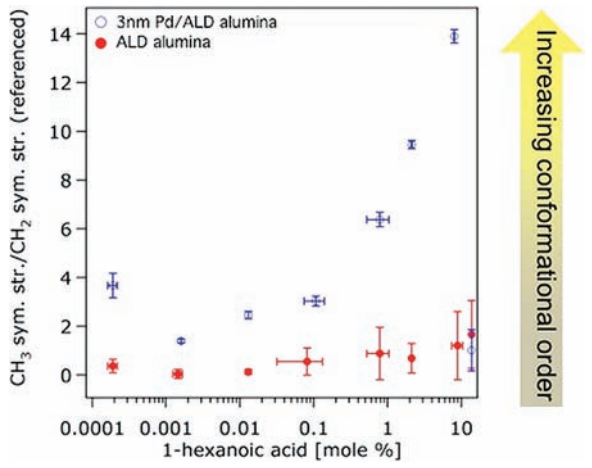

Figure 5. Ratio between CH_3 symmetric stretch and CH_2 symmetric stretch of 1-hexanoic acid adsorbed from liquid cyclohexane-d_{12} solutions onto ALD alumina with 3 nm Pd/ALD alumina (empty blue circles) and ALD alumina (filled red circles), each as a function of 1-hexanoic acid mol %. Signal for each experiment is referenced to the ratio at 0 mol %. Vertical error bars represent the propagation of one standard deviation in the ratio from the several repetitions of the experiment after referencing to the signal present under pure cyclohexane-d_{12}, while horizontal error bars depict one standard deviation in the concentrations, if they were different among trials.

alumina surface scales with the polarizability of the aluminum atom,[20,91] which often results in increased binding affinity for that site,[92] it is likely that hexanoic acid molecules interact more strongly with hydroxyl groups bonded to aluminum atoms adjacent to Pd nanoparticles than with aluminum atoms that are far away from them. Other forces may promote interaction with palladium particles that could result in conformational disorder, including the attractive interaction via dispersion forces between the hexanoic acid alkyl tails and the Pd nanoparticles or possibly partial back-bonding interactoins.[93−97] These interactions could lead to the observed differences in molecular ordering observed for the ALD alumina surface in the presence and absence of Pd nanoparticles, while not drastically changing the observed binding constant due to the relatively low density of these sites. If these sites were located at the junction between alumina, the Pd nanoparticle, and the solvent, then the number of strongly bound 1-hexanoic acid molecules would scale linearly with particle circumference. Providing qualitative support for this hypothesis is the observation that no significant changes in ordering with concentration are observed on surfaces with 1 nm rather than 3 nm palladium particles (Supporting Information), which have one-third as many nanoparticle perimeter sites; therefore, conformational disorder may be below detection limit. Future research could obtain quantitative confirmation that adsorption occurs at the nanoparticle parameter by measuring structures of adsorbed molecules on different surfaces containing particles of various sizes.

CONCLUSIONS

In conclusion, we have used synthetic surface chemistry and a variety of advanced characterization methods including nonlinear spectroscopy to demonstrate an example in which we bridge the gap between realistic complex catalyst materials and methods used to elucidate their surface chemistry, and do so at the liquid/solid interface. SFG was used as a tool for determining the adsorption behavior of 1-hexanoic acid on supported palladium nanoparticle surfaces prepared by ALD, which has recently emerged as a method for controlled catalyst synthesis. By utilizing the conformal deposition afforded by ALD, thin oxide films were prepared with supported palladium nanoparticles of defined size on flat surfaces amenable to study at the organic liquid interface by coherent surface spectroscopy techniques such as SFG.

Adsorption of 1-hexanoic acid occurs on ALD alumina surfaces, and on ALD alumina surfaces with palladium nanoparticles. 1-Hexanoic acid becomes more ordered with increasing adsorbate concentration for surfaces containing 3 nm Pd particles, but molecular ordering does not increase with concentration for surfaces with smaller palladium particles or no palladium particles. Thus, even though adsorption isotherms do not indicate a significant role for palladium in modulating adsorption energy for 1-hexanoic acid, the palladium particles play a role in interacting with adsorbates to modulate their structures. Furthermore, 1-hexanoic acid has a much higher binding constant than 1-hexanol and leads to its displacement in competitive adsorption experiments. Since carboxylic acids are known to be overoxidation products of selective oxidation reactions, their relative binding strengths in relation to those of alcohols is important for predicting catalytic reaction rates and catalyst poisoning due to site-blocking. For instance, the relatively low bulk concentration at which 1-hexanoic acid displaces 1-hexanol could be another factor explaining why oxidation, specifically of primary saturated alcohols, must be conducted at low conversions in order to obtain good selectivity.[3] The synergistic effects of adsorbate binding strength and the molecular structures they adopt on catalysts containing metal nanoparticles supported on oxides may lead to catalyst deactivation through poisoning sites on the support.

ASSOCIATED CONTENT

Supporting Information. Particle size and coverage, grazing incidence X-ray diffraction, SFG signals on α-Al_2O_3, ALD alumina and ALD alumina with 3 nm palladium particles with no added adsorbates, X-ray photoelectron spectroscopy of ALD alumina with 3 nm palladium particles, and a similarly prepared 50 cycle Pd film, CH_3 and CH_2 symmetric stretching amplitudes as a function of 1-hexanoic acid concentration, SFG signals from Pd films prepared by 50 cycles Pd ALD and by electron beam under 1-hexanoic acid solutions, SFG signals from 1-hexanoic acid adsorbed to α-Al_2O_3, 1-cycle ALD alumina and 10-cycle ALD alumina surfaces, SFG spectra of 1-hexanol adsorbed to ALD alumina and ALD alumina with 3 nm palladium particles, and GIXRD of samples after exposure. This material is available free of charge via the Internet at http://pubs.acs.org.

AUTHOR INFORMATION

Corresponding Author
geigerf@chem.northwestern.edu

ACKNOWLEDGMENT

We gratefully acknowledge helpful discussions with Professor Christopher Williams and Shuai Tan of the University of South Carolina, Dr. Jeffory Elam of Argonne National Laboratory, and Dr. Dragos Seghete, Lauren Kreno, and Alon Danon, of Northwestern University. We also acknowledge Dr. Jerry Carsello of

Northwestern University's J.B. Cohen X-ray Diffraction Facility for training, guidance, and helpful discussions, as well as the use of the Cohen Facility. Furthermore, we gratefully acknowledge Xinqui Chen and the Keck-II center at the Northwestern University Atomic and Nanoscale Characterization Experimental Center (NUANCE) for training and guidance as well as the use of the XPS instrument. Work involving SFG was supported by the Northwestern University Institute for Catalysis in Energy Processes which is funded by the Chemical Sciences, Geosciences, and Biosciences Division, Office of Basic Energy Sciences, Office of Science, U.S. Department of Energy (DE-FG02-03- ER15457) and the National Science Foundation Division of chemical, bioengineering, environmental and transport systems, catalysis and biocatalysis CBET program (Grant #0931701). This material is based upon work supported as part of the Institute for Atom-Efficient Chemical Transformations (IACT), an Energy Frontier Research Center funded by the U.S. Department of Energy, Office of Science, and Office of Basic Energy Sciences. This work made use of the J.B. Cohen X-ray Diffraction Facility supported by the MRSEC program of the National Science Foundation (DMR-0520513) at the Materials Research Center of Northwestern University. We also thank Spectra Physics, a Division of Newport Corporation, for equipment loans and donations as well as superb technical support. F.M.G. gratefully acknowledges support from an Irving M. Klotz professorship in physical chemistry.

REFERENCES

(1) Ayude, A.; Cechini, J.; Cassanello, M.; MartÌnez, O.; Haure, P. *Chem. Eng. Sci.* **2008**, *63*, 4969.
(2) Hussein, F. H.; Rudham, R. *J. Chem. Soc., Faraday Trans.* **1987**, *83*, 1631.
(3) Jenzer, G.; Schneider, M. S.; Wandeler, R.; Mallat, T.; Baiker, A. *J. Catal.* **2001**, *199*, 141.
(4) Keresszegi, C.; Ferri, D.; Mallat, T.; Baiker, A. *J. Phys. Chem. B* **2004**, *109*, 958.
(5) Mallat, T.; Baiker, A. *Chem. Rev. (Washington, DC, U.S.)* **2004**, *104*, 3037.
(6) Beier, M. J.; Hansen, T. W.; Grunwaldt, J.-D. *J. Catal.* **2009**, *266*, 320.
(7) Mitsudome, T.; Mikami, Y.; Ebata, K.; Mizugaki, T.; Jitsukawa, K.; Kaneda, K. *Chem. Commun. (Cambridge, U. K.)* **2008**, 4804.
(8) Stuchinskaya, T. L.; Kozhevnikov, I. V. *Catal. Commun.* **2003**, *4*, 417.
(9) Huber, G. W.; Chheda, J. N.; Barrett, C. J.; Dumesic, J. A. *Science* **2005**, *308*, 1446.
(10) Huber, G. W.; Cortright, R. D.; Dumesic, J. A. *Angew. Chem., Int. Ed.* **2004**, *43*, 1549.
(11) Huber, G. W.; Dumesic, J. A. *Catal. Today* **2005**, *111*, 119.
(12) Roman-Leshkov, Y.; Barrett, C. J.; Liu, Z. Y.; Dumesic, J. A. *Nature* **2007**, *447*, 982.
(13) Moreau, C.; Durand, R.; Razigade, S.; Duhamet, J.; Faugeras, P.; Rivalier, P.; Ros, P.; Avignon, G. *Appl. Catal., A* **1996**, *145*, 211.
(14) Schalow, T.; Brandt, B.; Starr, D. E.; Laurin, M.; Shaikhutdinov, S. K.; Schauermann, S.; Libuda, J.; Freund, H. J. *Phys. Chem. Chem. Phys.* **2007**, *9*, 1347.
(15) Baumer, M.; Libuda, J.; Neyman, K. M.; Rosch, N.; Rupprechter, G.; Freund, H.-J. *Phys. Chem. Chem. Phys.* **2007**, *9*, 3541.
(16) Somorjai, G. A. *J. Phys. Chem. B* **2000**, *104*, 2969.
(17) Ertl, G. *Angew. Chem., Int. Ed.* **2008**, *47*, 3524.
(18) Somorjai, G. A.; Aliaga, C. *Langmuir* **2010**, *26*, 16190.
(19) Rekoske, J. E.; Barteau, M. A. *Ind. Eng. Chem. Res.* **2011**, *50*, 41.
(20) van den Brand, J.; Blajiev, O.; Beentjes, P. C. J.; Terryn, H.; de Wit, J. H. W. *Langmuir* **2004**, *20*, 6308.
(21) Allara, D. L.; Nuzzo, R. G. *Langmuir* **1985**, *1*, 45.
(22) Foster, T. T.; Alexander, M. R.; Leggett, G. J.; McAlpine, E. *Langmuir* **2006**, *22*, 9254.
(23) Cervini-Silva, J.; Sposito, G. *Environ. Sci. Technol.* **2002**, *36*, 337.
(24) Buchbinder, A. M.; Weitz, E.; Geiger, F. M. *J. Phys. Chem. C* **2010**, *114*, 554.
(25) Buchbinder, A. M.; Weitz, E.; Geiger, F. M. *J. Am. Chem. Soc.* **2010**, *132*, 14661.
(26) Hayes, P. L.; Keeley, A. R.; Geiger, F. M. *J. Phys. Chem. B* **2010**, *114*, 4495.
(27) Jin, R. Y.; Song, K.; Hase, W. L. *J. Phys. Chem. B* **2000**, *104*, 2692.
(28) Bolton, K.; Bosio; Hase, W. L.; Schneider, W. F.; Hass, K. C. *J. Phys. Chem. B* **1999**, *103*, 3885.
(29) Clegg, R. S.; Reed, S. M.; Smith, R. K.; Barron, B. L.; Rear, J. A.; Hutchison, J. E. *Langmuir* **1999**, *15*, 8876.
(30) Hameren, R. v.; Elemans, J. A. A. W.; Wyrostek, D.; Tasior, M.; Gryko, D. T.; Rowan, A. E.; Nolte, R. J. M. *J. Mater. Chem.* **2009**, *19*, 66.
(31) Pallas, N. R.; Pethica, B. A. *Phys. Chem. Chem. Phys.* **2009**, *11*, 5028.
(32) Doyaguez, E. G.; Calderon, F.; Sanchez, F.; Fernandez-Mayoralas, A. *J. Org. Chem.* **2007**, *72*, 9353.
(33) Khodadadi-Moghaddam, M.; Habibi-Yangjeh, A.; Gholami, M. R. *J. Mol. Catal. A: Chem.* **2009**, *306*, 11.
(34) Ma, Z.; Zaera, F. *J. Phys. Chem. B* **2004**, *109*, 406.
(35) Somorjai, G. A.; Park, J. Y. *Angew. Chem., Int. Ed.* **2008**, *47*, 9212.
(36) Tollner, K.; Popovitz-Biro, R.; Lahav, M.; Milstein, D. *Science* **1997**, *278*, 2100.
(37) Kacer, P.; Cerven, L. *Appl. Catal., A* **2002**, *229*, 193.
(38) Stokes, G. Y.; Chen, E. H.; Buchbinder, A. M.; Paxton, W. F.; Keeley, A.; Geiger, F. M. *J. Am. Chem. Soc.* **2009**, *131*, 13733.
(39) Kim, M.; Hohman, J. N.; Cao, Y.; Houk, K. N.; Ma, H.; Jen, A. K.-Y.; Weiss, P. S. *Science* **2011**, *331*, 1312.
(40) Ferri, D.; Bürgi, T.; Baiker, A. *Helv. Chim. Acta* **2002**, *85*, 3639.
(41) Miranda, P. B.; Shen, Y. R. *J. Phys. Chem. B* **1999**, *103*, 3292.
(42) Richter, L. J.; Petralli-Mallow, T. P.; Stephenson, J. C. *Opt. Lett.* **1998**, *23*, 1594.
(43) Voges, A. B.; Al-Abadleh, H. A.; Musorrafiti, M. J.; Bertin, P. A.; Nguyen, S. T.; Geiger, F. M. *J. Phys. Chem. B* **2004**, *108*, 18675.
(44) Zhu, X. D.; Suhr, H.; Shen, Y. R. *Phys. Rev. B: Condens. Matter* **1987**, *35*, 3047.
(45) Zhuang, X.; Miranda, P. B.; Kim, D.; Shen, Y. R. *Phys. Rev. B: Condens. Matter* **1999**, *59*, 12632.
(46) Lambert, A. G.; Davies, P. B.; Neivandt, D. J. *Appl. Spectrosc. Rev.* **2005**, *40*, 103.
(47) Karimi, B.; Zamani, A.; Clark, J. H. *Organometallics* **2005**, *24*, 4695.
(48) Brazdil, J. F. *Top. Catal.* **2006**, *38*, 289.
(49) Chen, K.; Bell, A. T.; Iglesia, E. *J. Phys. Chem. B* **2000**, *104*, 1292.
(50) Fu, G.; Yi, X.; Huang, C.; Xu, X. I. N.; Weng, W.; Xia, W.; Wan, H.-L. *Surf. Rev. Lett.* **2007**, *14*, 645.
(51) Resini, C.; Montanari, T.; Busca, G.; Jehng, J.-M.; Wachs, I. E. *Catal. Today* **2005**, *99*, 105.
(52) Wu, H.; Zhang, Q.; Wang, Y. *Adv. Synth. Catal.* **2005**, *347*, 1356.
(53) Karimi, B.; Abedi, S.; Clark, J. H.; Budarin, V. *Angew. Chem., Int. Ed.* **2006**, *45*, 4776.
(54) Mallat, T.; Baiker, A. *Catal. Today* **1994**, *19*, 247.
(55) Ferri, D.; Baiker, A. *Top. Catal.* **2009**, *52*, 1323.
(56) Feng, H.; Elam, J. W.; Libera, J. A.; Setthapun, W.; Stair, P. C. *Chem. Mater.* **2010**, *22*, 3133.
(57) Elam, J. W.; Zinovev, A.; Han, C. Y.; Wang, H. H.; Welp, U.; Hryn, J. N.; Pellin, M. J. *Thin Solid Films* **2006**, *515*, 1664.
(58) Dillon, A. C.; Ott, A. W.; Way, J. D.; George, S. M. *Surf. Sci.* **1995**, *322*, 230.
(59) Ott, A. W.; Klaus, J. W.; Johnson, J. M.; George, S. M. *Thin Solid Films* **1997**, *292*, 135.
(60) Goldstein, D. N.; McCormick, J. A.; George, S. M. *J. Phys. Chem. C* **2008**, *112*, 19530.
(61) Lu, J.; Stair, P. C. *Langmuir* **2010**, *26*, 16486.

(62) Lu, J.; Stair, P. C. *Angew. Chem., Int. Ed.* **2010**, *49*, 2547.
(63) Lu, J.; Stair, P. C. *Langmuir* **2010**, *26*, 16486.
(64) Shen, Y. R. *The Principles of Nonlinear Optics*; John Wiley & Sons: New York, 1984.
(65) Guyot-Sionnest, P.; Hunt, J. H.; Shen, Y. R. *Phys. Rev. Lett.* **1987**, *59*, 1597.
(66) Esenturk, O.; Walker, R. A. *J. Chem. Phys.* **2006**, *125*, 174701.
(67) Conboy, J. C.; Messmer, M. C.; Richmond, G. L. *Langmuir* **1998**, *14*, 6722.
(68) Weeraman, C.; Yatawara, A. K.; Bordenyuk, A. N.; Benderskii, A. V. *J. Am. Chem. Soc.* **2006**, *128*, 14244.
(69) Stanners, C. D.; Du, Q.; Chin, R. P.; Cremer, P.; Somorjai, G. A.; Shen, Y. R. *Chem. Phys. Lett.* **1995**, *232*, 407.
(70) Elam, J. W.; Groner, M. D.; George, S. M. *Rev. Sci. Instrum.* **2002**, *73*, 2981.
(71) Guyot-Sionnest, P.; Hunt, J. H.; Shen, Y. R. *Phys. Rev. Lett.* **1987**, *59*, 1597.
(72) Voges, A. B.; Stokes, G. Y.; Gibbs-Davis, J. M.; Lettan, R. B.; Bertin, P. A.; Pike, R. C.; Nguyen, S. T.; Scheidt, K. A.; Geiger, F. M. *J. Phys. Chem. C* **2007**, *111*, 1567.
(73) Stokes, G. Y.; Buchbinder, A. M.; Gibbs-Davis, J. M.; Scheidt, K. A.; Geiger, F. M. *Vib. Spectrosc.* **2009**, *50*, 86.
(74) Esenturk, O.; Walker, R. A. *J. Phys. Chem. B* **2004**, *108*, 10631.
(75) Brindza, M. R.; Ding, F.; Fourkas, J. T.; Walker, R. A. *J. Chem. Phys.* **2010**, *132*, 114701.
(76) Ding, F.; Zhong, Q.; Brindza, M. R.; Fourkas, J. T.; Walker, R. A. *Opt. Express* **2009**, *17*, 14665.
(77) Wind, R. A.; George, S. M. *J. Phys. Chem. A* **2009**, *114*, 1281.
(78) Goldstein, D. N.; George, S. M. *Thin Solid Films* **2011**, *519*, 5339.
(79) Schalow, T.; Brandt, B.; Starr, D.; Laurin, M.; Schauermann, S.; Shaikhutdinov, S.; Libuda, J.; Freund, H. J. *Catal. Lett.* **2006**, *107*, 189.
(80) Vajda, S.; Pellin, M. J.; Greeley, J. P.; Marshall, C. L.; Curtiss, L. A.; Ballentine, G. A.; Elam, J. W.; Catillon-Mucherie, S.; Redfern, P. C.; Mehmood, F.; Zapol, P. *Nat. Mater.* **2009**, *8*, 213.
(81) Abbet, S.; Judai, K.; Klinger, L.; Heiz, U. *Pure Appl. Chem.* **2002**, *74*, 1527.
(82) Sefler, G. A.; Du, Q.; Miranda, P. B.; Shen, Y. R. *Chem. Phys. Lett.* **1995**, *235*, 347.
(83) Nanjundiah, K.; Dhinojwala, A. *Phys. Rev. Lett.* **2005**, *95*, 154301.
(84) Bellamy, L. J. *The Infra-red Spectra of Complex Molecules*; John Wiley & Sons: New York, 1975.
(85) Roeges, N. P. G. *A Guide to the Complete Interpretation of Infrared Spectra of Organic Structures*; John Wiley & Sons: New York, 1994.
(86) Dollish, F. R.; Fateley, W. G.; Bentley, F. F. *Characteristic Raman Frequencies of Organic Compounds*; John Wiley & Sons: New York, 1974.
(87) Lu, R.; Gan, W.; Wu, B.-h.; Zhang, Z.; Guo, Y.; Wang, H.-f. *J. Phys. Chem. B* **2005**, *109*, 14118.
(88) Atkins, P.; de Paula, J. *Physical Chemistry*; 7th ed.; W. H. Freeman and Company: New York, 2002.
(89) Cirtiu, C. M.; Hassani, H. O.; Bouchard, N.-A.; Rowntree, P. A.; Ménard, H. *Langmuir* **2006**, *22*, 6414.
(90) Tan, S.; Sun, X.; Williams, C. T. In *22nd Meeting of the North American Catalysis Society Detroit*, MI, 2011, p P.
(91) Ammal, S. C.; Heyden, A. *J. Chem. Phys.* **2010**, *133*, 164703.
(92) Skotak, M.; Karpinski, Z.; Juszczyk, W.; Pielaszek, J.; Kepinski, L.; Kazachkin, D. V.; Kovalchuk, V. I.; d'Itri, J. L. *J. Catal.* **2004**, *227*, 11.
(93) Chihara, T. *J. Catal.* **1984**, *89*, 177.
(94) Morales, R.; Zaera, F. *J. Phys. Chem. C* **2007**, *111*, 18367.
(95) Somorjai, G. A.; Rupprechter, G. *J. Phys. Chem. B* **1999**, *103*, 1623.
(96) Kao, C.-L.; Madix, R. J. *Surf. Sci.* **2004**, *557*, 215.
(97) Pichugina, D.; Lanin, S.; Kovaleva, N.; Lanina, K.; Shestakov, A.; Kuz'menko, N. *Russ. Chem. Bull.* **2010**, *59*, 2039.